KEYNOTE

Flash photolysis study of a Friedel–Crafts alkylation. Reaction of the photogenerated 9-fluorenyl cation with aromatic compounds

Robert A. McClelland,*[a] Frances L. Cozens,[a] Jianhui Li[a] and Steen Steenken[b]

[a] *Department of Chemistry, University of Toronto, Toronto, Ontario M5S 1A1, Canada*
[b] *Max-Planck-Institut fur Strahlenchemie, D-4330 Mulheim, Germany*

A combination of flash photolysis and product analysis is employed to investigate the reaction of aromatic compounds (ArH) with the 9-fluorenyl cation (Fl^+) photogenerated from 9-fluorenol in 1,1,1,3,3,3-hexafluoroisopropyl alcohol (HFIP). The availability of the photochemical route to Fl^+ means that the reaction of a benzylic-type cation with ArH can be directly followed by flash photolysis. An additional feature with electron-rich ArH is that the cyclohexadienyl cation is observed to grow as Fl^+ decays. Thus both cationic intermediates of a Friedel–Crafts alkylation are observed in the same experiment. The formation of the cyclohexadienyl cation is demonstrated to be reversible, or at least quasi-reversible, with the kinetic analysis furnishing absolute rate constants for the formation of this cation, as well as for its loss of H^+ and Fl^+. Values of $k_H:k_D$ for benzene: [$^2H_6$]benzene and toluene: [$^2H_8$]toluene are ~1.5 and demonstrate that Fl^+ addition is at least partly reversible with these compounds as well. The Hammett ρ^+ value obtained for a series of the less electron-rich ArH is −8, indicative of a transition state with considerable cyclohexadienyl cation character. Anisole shows a negative deviation from the Hammett correlation line, explained by the addition of Fl^+ to ArH becoming encounter-controlled. This behaviour is dramatically illustrated in a comparison of data for Fl^+ and Br_2. For the less electron-rich ArH, rate constants for the two electrophiles are parallel. However, from *m*-xylene through pentamethylbenzene, the rate with Fl^+ is unchanged, while the rate with Br_2 increases over 1000-fold. The concept of encounter control with Fl^+ is strongly supported by the absolute rate constants, which for the the electron-rich ArH are all in the range 1–2 × 10^9 dm^3 mol^{-1} s^{-1}, a magnitude typical of diffusion-controlled reactions. The electron-rich ArH also show no intermolecular selectivity since their reactions are encounter-controlled, but have a high intramolecular selectivity. It is suggested that a factor influencing the latter is the reversibility of formation of the cyclohexadienyl cation from the encounter complex.

Introduction

There has been a continuous interest in the reactivity of carbocations when formed as intermediates of reactions such as S_N1 solvolysis, electrophilic alkene addition, electrophilic aromatic substitution and cationic alkene polymerization. Of especial concern has been the selectivity of such intermediates when faced with a choice of nucleophiles. The classic method for examining this question has involved competition kinetics, whereby the cation forms in a slow step of some reaction and then partitions between two nucleophiles. With appropriate controls this provides a ratio of rate constants calculated from the ratio of products.[1,2] Similar rate constant ratios can be obtained from the kinetic analysis of common-ion inhibition. A more recent development has been the conversion of these rate constant ratios to absolute rate constants.[3,4] The assumption behind this is that one of the pair of nucleophiles is reacting at the diffusion limit. Azide ion has been the 'clock' nucleophile most commonly employed.

Both competition kinetics and common-ion inhibition provide kinetic information indirectly in that the cation is not actually seen as the reaction proceeds. A large number of carbocations have of course now been directly observed under stable ion conditions.[5] The strongly acidic nature of these conditions however normally precludes the measurement of rate constants for the reactions with added nucleophiles, since these are rendered unreactive by protonation.

Flash photolysis offers an alternative approach for the observation of carbocations, and in this case detailed kinetic information can be readily obtained. The basis of the technique is the use of a short pulse of light to initiate a photochemical reaction that results in the cation. This is directly observed, normally with absorption spectroscopy, and the kinetics of its reactions followed over a short period of time. As demonstrated principally by studies reported in the last 10 years, a variety of carbocations can be studied in this way.[6,7] Most of these can be classified as being either of the 'benzylic-type' or of the 'cyclohexadienyl-type'. Such cations have a UV–VIS chromophore and are thus able to be detected. An example in the first category is the diphenylmethyl cation, observed in 2,2,2-trifluoroethanol (TFE) following photoheterolysis of an acetate or *p*-cyanophenolate precursor [reaction (1)].[8,9] In the second category lies the 2,4,6-trimethylbenzenium ion, generated by

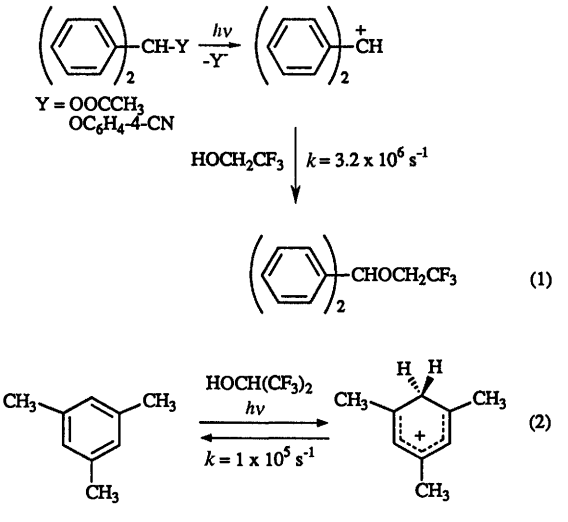

photoprotonation of mesitylene in 1,1,1,3,3,3-hexafluoroisopropyl alcohol (HFIP) [reaction (2)].[10]

As is evident from these examples, the solvents that have been employed are themselves reactive (water, simple alcohols and acetonitrile) and the absolute rate constant for the decay of the cation in the solvent alone is one kinetic parameter that is readily obtained. These solvents also permit the addition of quenching nucleophiles (or bases) and thus provide for the direct measurement of the rate constants for the cation : nucleophile combination (or deprotonation) as well. This technique, for example, has been employed to provide absolute rate constants for the reaction of azide ion with several classes of cation.[11,12] As assumed in the 'azide-clock' approach, this reaction is indeed diffusion limited, at least for cations that are reasonably reactive.

The cation that forms the subject of this article is the 9-fluorenyl cation (Fl^+). The photochemical precursor in this case is the alcohol, 9-fluorenol. This system illustrates an interesting feature of photochemical routes to carbocations, namely that there is often a significant difference compared with an analogous ground state reaction. The initial studies were carried out by Wan and Krogh who found that 9-fluorenol undergoes a relatively efficient reaction on irradiation in aqueous methanol resulting in the production of 9-methoxyfluorene [reaction (3)].[13,14] This substitution was proposed to

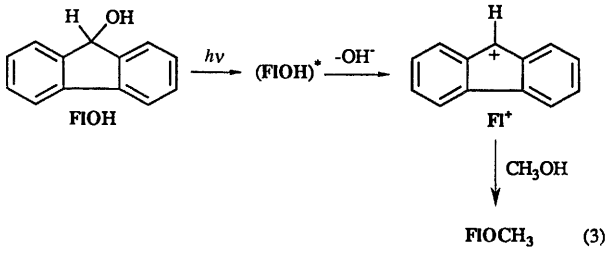

(3)

occur *via* C–OH heterolysis of the singlet excited state of the alcohol leading to the 9-fluorenyl cation, followed by trapping with methanol. This heterolysis occurs despite the poor leaving group, the hydroxide ion. Alcohols such as diphenylmethanol that lack the central ring of the fluorenyl system do not undergo this photoreaction, or do so considerably less efficiently. This led to the proposal that Fl^+ forms in the fluorenyl systems because of an enhanced reactivity of excited states leading to internal cyclic arrays containing $4n$–π systems.[13-15]

The facile formation of Fl^+ is surprising with respect not only to the poor leaving group, but also in that these types of cations are somewhat destabilized in the ground state. This can be seen in solvolysis reactions proceeding *via* 9-fluorenyl cations that occur several orders of magnitude more slowly than those of analogues lacking the central ring.[16-18] A comparison of equilibrium pK_R data also shows the effect, 9-phenyl-9-fluorenyl, $pK_R = -10.8$,[19] *versus* triphenylmethyl, $pK_R = -6.6$,[20,21] and Fl^+, $pK_R = -17.3$,[22] *versus* diphenylmethyl, $pK_R = -13.3$.[20] The parent Fl^+ has not been observed in concentrated acid or super acids,[23] and the pK_R value is an estimate from electrochemical measurements.[22]

Initial flash photolysis studies with 9-fluorenol were carried out by Mecklenburg and Hilinski.[24] These workers found that Fl^+ is extremely short-lived in aqueous solution, forming and decaying within the laser pulse in a picosecond apparatus (lifetime < 25 ps). With the less nucleophilic HFIP as solvent, the lifetime increases by over six orders of magnitude to 10 μs.[25] As shown in Table 1 the diphenylmethyl cation is longer lived in each solvent, by two to three orders of magnitude. A similar difference is seen in comparing the 9-phenyl-9-fluorenyl cation with its analogue, the triphenylmethyl cation. Thus the reactivities of 9-fluorenyl cations also reflect a destabilization relative to similar cations lacking the central ring. Recent theoretical calculations have suggested that this destabilization

Table 1 Rate constants for the decay of cations in water and alcohol solvents[a]

Cation	$k_s(H_2O)/s^{-1}$	$k_s(TFE)/s^{-1}$	$k_s(HFIP)/s^{-1}$
Triphenylmethyl	1.5×10^5 [b]		
9-Phenyl-9-fluorenyl	1.5×10^7 [c]	1.5×10^4 [c]	
Diphenylmethyl	1.3×10^9 [d]	3.2×10^6 [e]	$\sim 1 \times 10^1$ [f]
9-Fluorenyl	$>4 \times 10^{10}$ [g]	8×10^8 [h]	1×10^5 [i]
Cumenyl			9×10^3 [j]
Phenethyl			6×10^5 [j]

[a] Temperature 20 °C. [b] Ref. 26. [c] Ref. 27. [d] Ref. 28. [e] Ref. 8. [f] R. A. McClelland and S. Steenken, unpublished results. [g] Ref. 24. [h] E. F. Hilinski, personal communication. [i] Ref. 25. [j] Ref. 29.

is not associated with anti-aromatic character, but can be accounted for by a combination of a smaller amount of π-stabilization coupled with van der Waals and ring strain.[30]

As is apparent from the data in Table 1, the solvent HFIP has a dramatic kinetic stabilizing effect. This has been exploited to observe a number of cations that are relatively reactive and, consequently, are very short lived in solvents such as water, methanol and ethanol. The 9-fluorenyl cation has a reactivity towards the solvent HFIP that lies between that of the cumenyl cation and the phenethyl cation.

This combination of a reactive cation and a weakly nucleophilic solvent suggested the possibility that weak π-nucleophiles such as benzene and other aromatic compounds (ArH) might compete with the solvent resulting in a Friedel–Crafts alkylation. With flash photolysis, the step in that process where the carbocation reacts with the aromatic compound could then be directly observed. This does turn out to be the case, as we have reported in a preliminary form.[31] In this paper we present full details of this study, which involves a combination of flash photolysis and product studies to delineate the mechanistic details. In addition to the reactivity aspects mentioned above, the Fl^+–HFIP system has other advantages for the study of photoinitiated Friedel–Crafts reactions. As will be seen, the photochemistry is very clean, with no side-reactions to complicate product analyses. Importantly, 9-fluorenol has absorbance at wavelengths greater than 300 nm. This means that the Fl^+ precursor can be selectively excited in the presence of high concentrations of ArH that do not absorb above 300 nm.

Results and Discussion

Quenching by benzene and toluene

The 9-fluorenyl cation has λ_{max} at 515 nm,[24,25] and our initial experiments were carried out at this wavelength, generating the cation by 308 nm laser excitation of 9-fluorenol. In HFIP alone, the cation decays with good single exponential kinetics, with a first-order rate constant as given in Table 1. The decay remains first-order when benzene and toluene are added, but the rate constant is greater. The expected linear relation in [ArH] is observed. The slope, $k_{Ar}(obs)$, is the second-order rate constant for quenching by the aromatic compound. Values are 3.3×10^5 $dm^3\ mol^{-1}\ s^{-1}$ for benzene, and 1.1×10^7 $dm^3\ mol^{-1}\ s^{-1}$ for toluene.

Products with benzene and toluene

The only product observed on irradiation of 9-fluorenol in HFIP alone is the ether **1** (Scheme 1). This forms in quantitative yield, even for irradiation times that correspond to >95% conversion. This contrasts with the situation with methanol as the trapping solvent, where the ether product, 9-methoxyfluorene, undergoes photohomolysis to the 9-fluorenyl radical, resulting in fluorene and 9,9′-bifluorene as products.[13,14] This secondary photolysis consumes the ether as soon as substantial amounts are present, so that the maximum chemical yield is 30%. In HFIP there is no detectable fluorene or

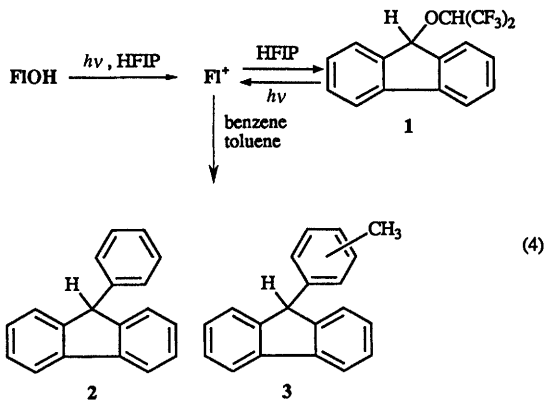

Table 2 Relation between the ratio [**2**]:[**1**] and irradiation time for the 300 nm photolysis of 9-fluorenol (10^{-3} mol dm^{-3}) in HFIP in the presence of 1 mol dm^{-3} benzene

Irradiation time/min	% Conversion of 9-fluorenol	[2]:[1]
3	16	1.82
6	28	1.82
10	42	1.79
14	49	1.79
20	68	2.01
30	87	2.13

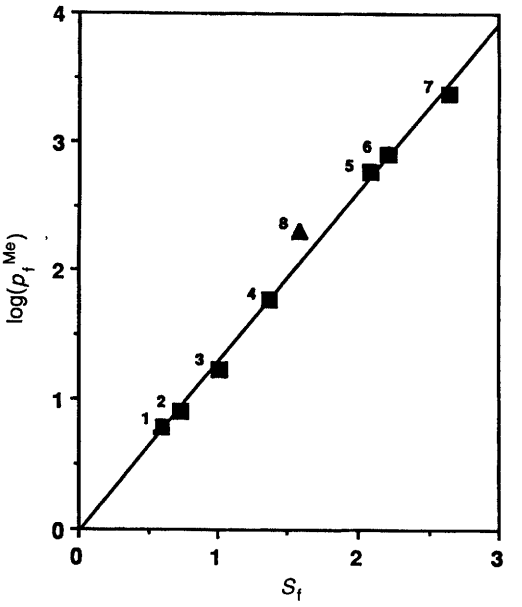

Fig. 1 Relation between intermolecular and intramolecular selectivity in electrophilic substitutions in toluene. Data for points **1**–**7** are from ref. 33, and represent **1**: ethylation (EtBr, $GaBr_3$), **2**: methylation (MeBr, $AlBr_3$), **3**: mercuration [$Hg(OAc)_2$, HOAc], **4**: bromination (HOBr, $HClO_4$), **5**: benzoylation (PhCOCl, $AlCl_3$), **6**: chlorination (Cl_2, HOAc), **7**: bromination (Br_2, HOAc). Point **8** represents the 9-fluorenyl cation in HFIP.

9,9′-bifluorene (less than 0.1%) even on prolonged irradiation. The stability of **1** towards photohomolysis was confirmed by irradiating an authentic sample for a time that would result in essentially complete reaction of the alcohol precursor. The ether was recovered unchanged.

When benzene was added an additional product was observed whose GC–MS suggested (9-fluorenyl)benzene (**2**). This was verified by an independent synthesis of this material through the reaction of phenylmagnesium bromide with fluorenone, followed by reduction of the so-formed alcohol. A similar procedure was followed for the preparation of a number of the substitution products. In the case of substituted ArH these syntheses not only provide an authentic sample, but unambiguously answer questions of regiochemistry.

Quantitative analyses were performed by GC, employing the authentic materials as standards. An observation that was made with all systems is illustrated with data for benzene in Table 2. Only the ether and the aromatic substitution product(s) are formed, and for irradiation times corresponding to less than 40–50% conversion, their ratio is constant within experimental error. On prolonged irradiation however, the relative yield of the substitution product increases. Our explanation is that the ether is undergoing photoheterolysis to regenerate the 9-fluorenyl cation. This photochemistry is invisible in experiments with no added benzene, since the cation is simply recaptured by the solvent. With benzene or another aromatic compound present, however, a fraction of the cation that forms from the ether is diverted to the aromatic substitution product. The result is an increase in the relative yield of this material.

Verification of this explanation was provided by flash photolysis experiments with the authentic ether. This indeed shows a signal corresponding to Fl^+, albeit a much weaker signal than the one seen with 9-fluorenol under identical conditions.

With toluene, all three substitution products **3** are formed, in amounts of 5.2 ± 0.2% *ortho*, 4.7 ± 0.2% *meta* and 90.1 ± 0.4% *para*. These relative yields are independent of the concentration of toluene. They are also unchanged on prolonged irradiation, despite the previously discussed increase in their total yield relative to the ether **1**. This *ortho*:*meta*:*para* ratio is typical of alkylations of toluene. The relatively small amount of the *ortho* product is likely to be a consequence of steric hindrance.[32]

The *para*:*meta* ratio provides a value of S_f [$\log(p_f^{Me}:m_f^{Me})$[33]] of 1.58.

A competition experiment carried out with benzene and toluene both present results in a mixture of **2** and **3**, the latter in the same *ortho*:*meta*:*para* ratio as above. The ratio $k_{toluene}:k_{benzene}$ is 41, so that p_f^{Me}, the partial rate factor for *para* substitution in toluene, is 2.2×10^2. Brown and Stock have demonstrated that there is a correlation between the intramolecular selectivity factor S_f and the intermolecular selectivity as measured by $\log(p_f^{Me})$.[33] This relationship is shown in Fig. 1, with data for electrophiles selected from a considerably larger set. The point for the 9-fluorenyl–HFIP system does lie slightly above the line that provides the best fit to the overall data. However, an examination of the plot that includes all of the electrophiles[33] reveals that there is scatter. The point for Fl^+ lies well within this scatter. The conclusion is that Fl^+ is reacting as a typical electrophile. In comparison with other electrophiles reacting with benzene and toluene, Fl^+ exhibits intermediate selectivity.

The 9-fluorenyl cation was also generated thermally in HFIP through the ionization of 9-bromofluorene. In a competition experiment with toluene and benzene, $k_{toluene}:k_{benzene} = 43$, and *ortho*:*meta*:*para* = 4.5:5.5:90. These are the same results as obtained from the photochemical reaction and provide evidence that the latter reaction does involve the same ground state cation as formed in the ionization.

Products with anisole

With anisole as the trapping compound, the *para* and *ortho* isomers **6** and **7** are obtained, in a 45:55 ratio (Scheme 2). There is less than 0.1% of the *meta* isomer, as verified by coinjection of an authentic sample. The relatively large amount of *ortho* product contrasts with the situation with toluene, but has been observed in other studies involving anisole.[34–37] Kovacic and Hiller, for example, found a 40:60 *para*:*ortho* ratio in the alkylation of anisole with $(CH_3)_2CHCl$ and $AlCl_3$.[35] These workers attributed the relatively large amount of *ortho* product to an initial oxygen alkylation followed by intramolecular rearrangement. Such a rearrangement has however been criticized because of the requirement for a transition state with a four-membered ring.[36] Two studies have shown that the

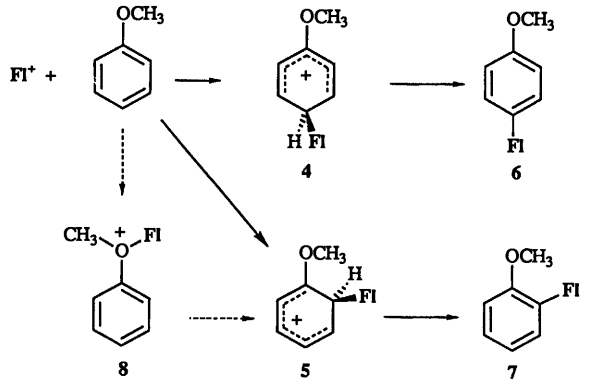

Scheme 2

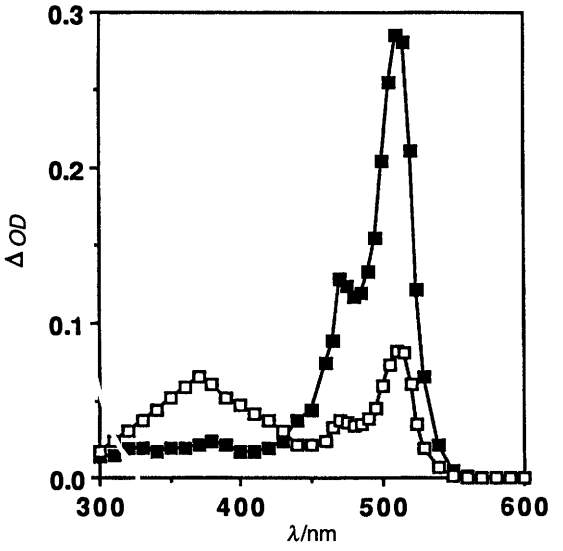

Fig. 2 Transient absorption spectra following 308 nm excitation of 9-fluorenol in HFIP in the presence of 3×10^{-3} mol dm^{-3} anisole. Spectra were recorded at times of 20 ns (■) and 400 ns (□) after the laser pulse.

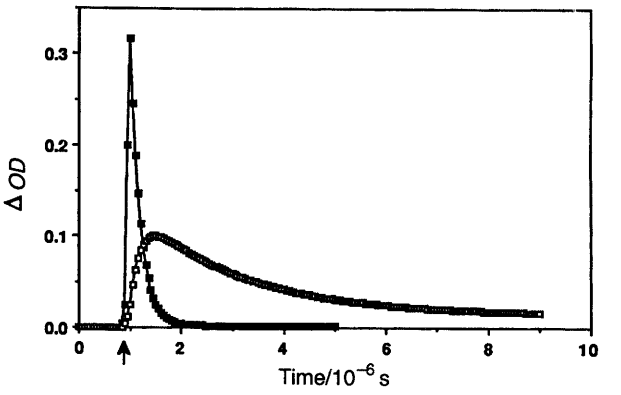

Fig. 3 Absorbance changes at 515 nm (■) and 370 nm (□) following 308 nm excitation of 9-fluorenol in HFIP in the presence of 3×10^{-3} mol dm^{-3} anisole. The arrow indicates the laser pulse.

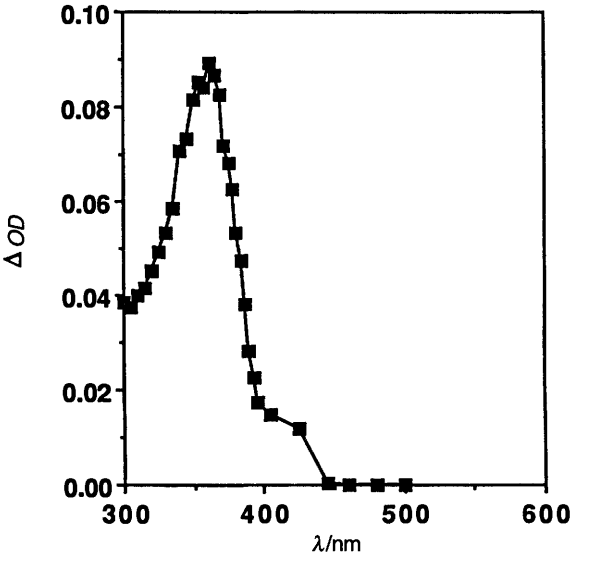

Fig. 4 Transient absorption spectrum following 248 nm excitation of anisole in HFIP

dimethylphenyloxonium ion is present in the methylation of anisole, but that the subsequent methyl transfer to the ring is an intermolecular process.[36,37]

The oxonium ion that would form with Fl^+ is **8**. In a subsequent section we will show that flash photolysis provides direct information on the possible presence of this species. In terms of the product analyses, it can be noted that if **8** does form and then react with a second anisole, the methyl group might transfer. This clearly does not happen, since there is no methoxytoluene (*ortho* or *para*).

Quenching by anisole

There are two features of the flash photolysis experiments with anisole present that distinguish this system from benzene and toluene. The first is a very large value of $k_{anisole}$(obs), 1.7×10^9 dm^3 mol^{-1} s^{-1}, meaning that much lower concentrations suffice to provide significant acceleration to the decay of Fl^+. The second, and more interesting observation, relates to the presence of a second transient. In the experiments with benzene and toluene, the transient spectra at various times are no different from those seen in the absence of benzene and toluene, except in the quantitative sense that the decay is more rapid when the aromatic compound is present. With anisole however, a new transient appears as Fl^+ decays, with the rate of growth the same as the rate of decay (Figs. 2 and 3). The implication is that this new species is a product of the reaction of Fl^+ and anisole. To assign this species we will first discuss the results of experiments involving the irradiation of anisole on its own.

Photoprotonation of anisole in HFIP

As shown in reaction (2) above, HFIP is sufficiently acidic to protonate excited aromatic compounds, forming cyclohexadienyl cations that are observed by flash photolysis.[10,38–41] The result with anisole is a transient with λ_{max} at 360–365 nm, as shown in Fig. 4. This species can be identified as the 2-methoxybenzenium ion **9**, formed on photoprotonation at the 2-position of anisole (Scheme 3).

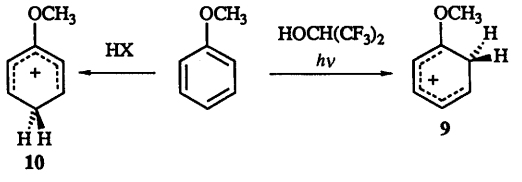

Scheme 3

Evidence that this species is a cyclohexadienyl cation is its quenching by added alcohols and bromide, but not by oxygen. Moreover the reactivity pattern, MeOH ~ EtOH ~ Pr^{i}OH ~ Bu^{t}OH (Table 3), is typical of cyclohexadienyl cations where the quenching involves deprotonation.[10,41] Cations that react by nucleophilic addition show an order of magnitude decrease across this series.

Evidence for the structure as the regioisomer **9** comes from experiments in $(CF_3)_2CHOD$, followed by isolation and ^1H NMR spectroscopy. The anisole is recovered quantitatively, but there is exchange of the C2 hydrogens.

Table 3 Rate constants for the reaction of the 1-(9-fluorenyl)-2-methoxybenzenium ion (**5**), generated by the reaction of the 9-fluorenyl cation with anisole in HFIP and the 2-methoxybenzenium ion (**9**), generated by photoprotonation of anisole in HFIP

Reagent	k(**5**)[a]	k(**9**)[a]
$(CF_3)_2CHOH$	5.9×10^5	6.6×10^5
CH_3OH	6.9×10^6	2.2×10^7
CH_3CH_2OH	6.7×10^6	1.9×10^7
$(CH_3)_2CHOH$	6.4×10^6	2.0×10^7
$(CH_3)_3COH$	5.2×10^6	1.9×10^7
Br^-	3.9×10^9	4.9×10^9

[a] Units are $dm^3\ mol^{-1}\ s^{-1}$ except for the solvent where the units are s^{-1}; 20 °C.

Table 4 Absorption maxima of cyclohexadienyl cations obtained by addition of the 9-flourenyl cation and H^+ to alkylbenzenes

Substituents	λ_{max}(FlArH$^+$)[a]/nm	λ_{max}(HArH$^+$)[b]/nm
1,3-Me_2	340	330[c,d]
1,2,3-Me_3	375	365[c,d]
1,2,4-Me_3	365	355[c,d]
1,3,5-Me_3	370	355,[c,e] 355[f,g]
1,2,3,4-Me_4	380	370[c,d]
1,2,3,5-Me_4	380	365[c,d]
Me_5	390	380,[c,d] 377[f,h]
1,3,5-Et_3	380	360[c,d]
1,3,5-iPr_3	380	365[c,d]

[a] Cyclohexadienyl cation derived from addition of Fl^+. [b] Protonated aromatic compound. [c] In HFIP, generated by photoprotonation. [d] This work. [e] Ref. 10. [f] Obtained by thermal protonation in strong acids. [g] Ref. 43. [h] Ref. 44.

The assignment to **9** is also consistent with a value for λ_{max} calculated with an empirical equation that uses the parent benzenium ion λ_{max} as a reference, with positive or negative $\Delta\lambda$ values for substitutions.[38] This treatment predicts a λ_{max} for **9** of 372 nm, well within the range of that observed, especially considering the uncertainties in this analysis. The most likely alternative structure is of course the 4-methoxybenzenium ion (**10**). This cation has been obtained previously by protonating anisole in strong acids and it has a very different spectrum, with λ_{max} near 285 nm.[42]

The anisole–HFIP system is a further example of contrasting regiochemistries associated with protonation in the ground state and in the excited state. The 1,3-dimethoxybenzenes offer related examples.[38] Ground-state protonation occurs with these compounds at the 4-position, affording 2,4-dimethoxybenzenium ions, while photoprotonation occurs at the 2-carbon, giving the 2,6-dimethoxy isomers.

1-(9′-Fluorenyl)-2-methoxybenzenium ion (5)

The transient that grows in the reaction with Fl^+ and anisole clearly has a similar λ_{max} to the 2-methoxybenzenium ion, and thus can be assigned as the Fl^+ adduct **5**. In addition to the spectral analogy, the kinetics are also similar, as shown in the comparison in Table 3. The rate constants for the fluorenyl adduct are slightly smaller, possibly due to a steric effect associated with the larger substituent. The assignment to **5** is also consistent with the products, which show that *ortho*-alkylation does occur and in substantial yield. Substitution at the *para* position also occurs, but as discussed above the cyclohexadienyl cation of this process (**4**) is expected to absorb below 300 nm. This region is not accessible in the flash photolysis experiments due to absorbance by the precursors.

Presence of an oxonium ion intermediate?

Thus, both the initial 'alkyl' cation and the *ortho*-cyclohexadienyl adduct of a Friedel–Crafts alkylation are seen in the same flash photolysis experiment. This is a novel observation, and more importantly it provides a means for evaluating the possible presence of a third cation, the oxonium ion **8**. The kinetic scheme that applies if **8** were an intermediate is shown in reaction (4).

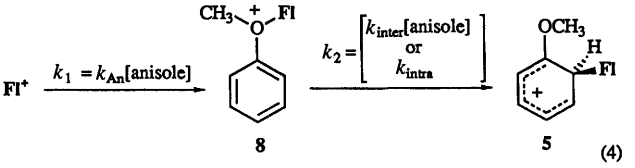

(4)

Under conditions where anisole is in large excess, two consecutive first-order reactions with rate constants k_1 and k_2 would lead from Fl^+ through **8** to the cyclohexadienyl cation. The second rate constant refers to the conversion of **8** to **5**, and as discussed above, this is written as potentially occurring by inter- or intra-molecular pathways.

The key experimental observation is that the appearance of **5** is first-order with a first-order rate constant identical to the one obtained for the disappearance of Fl^+. In kinetic terms this means that the rate constant being measured must be k_1, and k_2 must be larger than k_1, by at least a factor of 10. For the mechanism where **8**→**5** occurs by an intermolecular reaction, both k_2 and k_1 depend on [anisole]. Thus $k_2 \geqslant 10k_1$ requires $k_{inter} \geqslant 10k_{An}$. The absolute value for the latter however is known, since this is equal to $k_{anisole}$(obs) (see later). Thus $k_{inter} \geqslant 1.7 \times 10^{10}\ dm^3\ mol^{-1}\ s^{-1}$. This lower limit is greater than the rate constant for diffusional encounter of a neutral molecule and a cation in HFIP (see later). Thus such a mechanism cannot operate.

The intramolecular mechanism cannot be ruled out in the same way, but a lower limit of $\geqslant 10^8\ s^{-1}$ can be placed on the rate constant k_{intra}. This limit is established through experiments in which the anisole concentration is $\geqslant 0.1$ mol dm^{-3}. At these concentrations the decay of Fl^+ is so rapid that no signal can be observed on the $\geqslant 20$ ns timescale, the limit of our apparatus. At the same time, the cyclohexadienyl cation **5** is fully formed within the laser pulse. This means that the rate constant for the formation of **5** is $\geqslant 10^8\ s^{-1}$, providing the above lower limit for k_{intra}.

There is no evidence for **8** as an intermediate even at very short times. If **8** does form, it cannot transfer Fl^+ to a second molecule of anisole, since this requires a rate constant greater than that for diffusion. Even if the transfer is by an intramolecular mechanism, the rate constant must be greater than $10^8\ s^{-1}$. The conclusion therefore is that the maximum lifetime of **8** is 10 ns.

Quenching by benzenes bearing multiple alkyl substituents

Cyclohexadienyl cations are also observed with aromatic derivatives bearing two or more alkyl substituents in a 1,3 relation. Evidence for the assignment takes the same form as discussed with anisole, in particular the close similarity between the spectra obtained with Fl^+ and that of the protonated alkylbenzene. The latter cyclohexadienyl cations have been generated by photoprotonation in HFIP. In selected cases spectral data from strong acids are also available. The aromatic systems that have been investigated in this way are summarized in Table 4, along with a listing of λ_{max} values. In general the cations from Fl^+ absorb at a slightly higher λ_{max} value than the protonated analogue, the same observation as made with anisole.

There is however an important difference from anisole. With all of the alkylbenzenes in Table 4, the decay of Fl^+ is not a single exponential, but is two-component (Fig. 5). This behaviour is especially evident at the lower concentrations, but does continue even at higher concentrations. The two phases are well separated, except at very low aromatic concentrations ($< \sim 0.2$ mmol dm^{-3}). Thus the two kinetic components can be

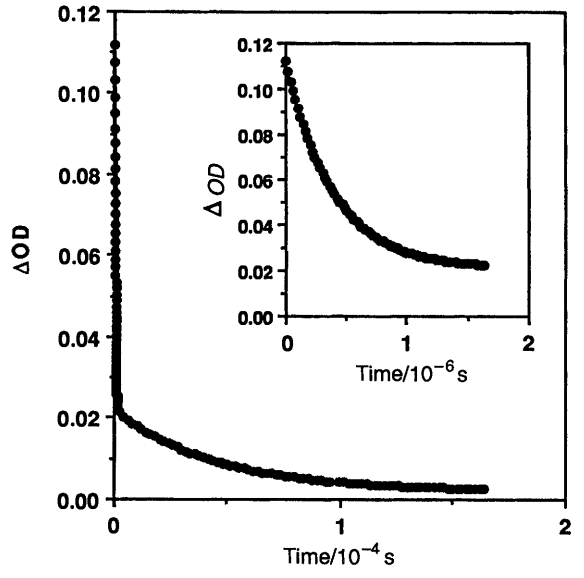

Fig. 5 Absorbance changes at 515 nm following 308 nm excitation of 9-fluorenol in HFIP in the presence of 2×10^{-3} mol dm^{-3} 1,3,5-triisopropylbenzene

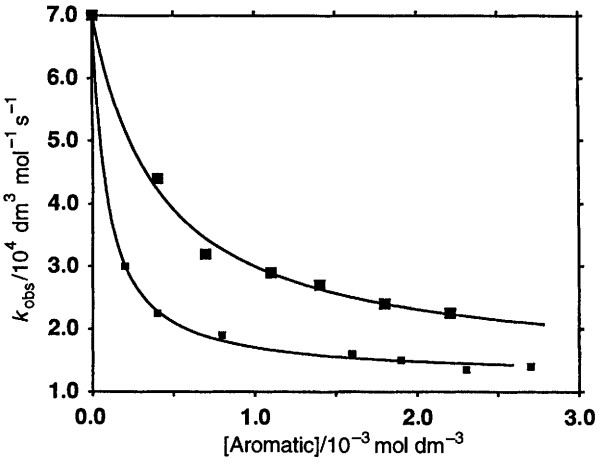

Fig. 6 Observed rate constant for the decay of the Fl^+:Fl–benzenonium equilibrium mixture as a function of the concentration of 1,3,5-triethylbenzene (small squares) and 1,3,5-triisopropylbenzene (large squares). The points are experimental; the curve has been drawn according to eqn. (6) using parameters given in Table 5.

separately analysed to provide two first-order rate constants. The initial rapid decay is accompanied by the appearance of the cyclohexadienyl cation. The first-order rate constants, defined as k_{fast}, are identical whether calculated from the decay or from the growth. The slow decay at 515 nm is actually accompanied by the decay of the cyclohexadienyl cation. Once again, the first-order rate constants, defined as k_{slow}, are identical. The constant k_{fast} follows a linear dependence in [ArH], while k_{slow} has a more complex dependence. Two examples of the latter behaviour are provided in Fig. 6.

These observations are consistent with a kinetic model where there is an initial process involving formation of an equilibrium between Fl^+ and the cyclohexadienyl cation. The establishment of this equilibrium corresponds to the fast decay of Fl^+ and the concomitant growth of the cyclohexadienyl cation. The slower process that follows then represents the decay of the equilibrating mixture. This can occur *via* two pathways, solvent addition to Fl^+ and solvent deprotonation of the cyclohexadienyl cation (Scheme 4).

For such a mechanism, k_{fast} represents the approach to the equilibrium position and is given by eqn. (5). This predicts a linear dependence of k_{fast} in [ArH], as is observed, with the

Table 5 Rate constants[a] for the formation, breakdown and deprotonation of cyclohexadienyl cations formed from the 9-fluorenyl cation and alkylbenzenes in HFIP

Substituent	k_f/10⁹ dm³ mol⁻¹ s⁻¹	k_r/10⁴ s⁻¹	k_d/10³ s⁻¹	$k_f:k_r$[b]/dm³ mol⁻¹	K_{eq}[c]/dm³ mol⁻¹
1,3-Me_2	1.1	97	500	1.1×10^3	1.8×10^3
1,2,4-Me_3	1.3	170	830	7.9×10^2	2.3×10^3
1,3,5-Me_3	1.9	6.0	34	3.3×10^4	4.1×10^4
1,2,3,4-Me_4	1.5	16	86	9.6×10^3	5.7×10^4
1,2,3,5-Me_4	1.7	4.4	8.7	3.8×10^4	1.4×10^4
Me_5	1.5	1.3	4.8	1.1×10^5	3.5×10^4
1,3,5-Et_3	1.8	17	8.5	1.1×10^4	1.2×10^4
1,3,5-iPr_3	1.3	57	12	2.3×10^3	5.2×10^3

[a] Temperature −20 °C. [b] Equilibrium constant determined kinetically as ratio of two rate constants. [c] Equilibrium constant obtained by absorbance method.

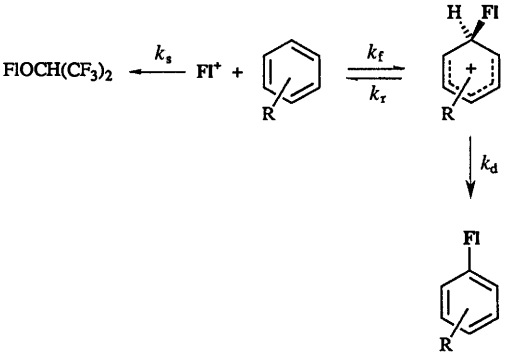

Scheme 4

$$k_{fast} = k_f[ArH] + k_r \quad (5)$$

slope of the plot providing k_f. The intercept would supply the rate constant k_r. However this could not be precisely measured because of the extrapolation required. As will be discussed, the equilibrium assumption is only approximate. This means that kinetic data must be obtained at reasonable concentrations of ArH so that the fast and slow processes are well separated. At lower concentrations where the intercept makes a greater contribution to k_{fast}, the two processes are not well separated and good kinetic data cannot be obtained.

The rate law that describes the slower reaction out of the Fl^+–cyclohexadienyl cation equilibrium is given in eqn. (6),

$$k_{slow} = \frac{k_s + k_d\left(\frac{k_f}{k_r}\right)[ArH]}{1 + \left(\frac{k_f}{k_r}\right)[ArH]} \quad (6)$$

where the ratio $k_f:k_r$ is the equilibrium constant. The observed values of k_{slow} were treated using this equation, by fixing the constants k_s and k_f as, respectively, the rate constant for Fl^+ decay in the absence of ArH and the slope of the fast component. The remaining k_r and k_d values were then evaluated from non-linear least squares fits. This procedure reproduces the experimental data, as shown by the agreement between the experimental points and the lines in Fig. 6.

Values for k_d, k_f and k_r are given in Table 5, and allow us to examine whether the equilibrium treatment is reasonable. For such a model, the reactions that occur within the equilibrium must be faster than the reactions that form stable products, *i.e.* $k_f[ArH] > k_s$ and $k_r > k_d$. With k_f being greater than 10^9 dm^3 mol^{-1} s^{-1} and $k_s \sim 10^5$ s^{-1}, the first inequality is satisfied once [ArH] exceeds 10^{-4} mol dm^{-3}. Table 5 shows that the second is also satisfied, with the value of $k_r:k_d$ being at least 2 in all the cases. However, for equilibration to be really complete before

Table 6 Rate constants and product distributions for the reaction of the 9-fluorenyl cation with aromatic compounds

Substs.	k_{Ar}(obs)/dm^3 mol^{-1} s^{-1}	Products
H	3.3×10^5	(9-Fluorenyl)benzene
F	7.9×10^5	Not determined
Ph	2.8×10^6	>95% *p*-(9-Fluorenyl)biphenyl
Me	1.1×10^7	5:5:95 *o*:*m*:*p*-(9-Fluorenyl)toluene
MeO	1.7×10^9	55: <0.1:45 *o*:*m*:*p*-(9-Fluorenyl)anisole
1,2-Me_2	2.3×10^8	~1% 3-(9-Fluorenyl)-1,2-dimethylbenzene 99% 4-(9-Fluorenyl)-1,2-dimethylbenzene
1,3-Me_2 [b]	3.7×10^8	0.5% 2-(9-Fluorenyl)-1,3-dimethylbenzene 99.5% 4-(9-Fluorenyl)-1,3-dimethylbenzene <0.1% 5-(9-Fluorenyl)-1,3-dimethylbenzene
1,4-Me_2	3.0×10^7	2-(9-Fluorenyl)-1,4-dimethylbenzene
1,3,5-Me_3 [b]	6.9×10^8	2-(9-Fluorenyl)-1,3,5-trimethylbenzene
Me_5 [b]	4.0×10^8	6-(9-Fluorenyl)-1,2,3,4,5-pentamethylbenzene

[a] Second-order rate constant for quenching of Fl^+ by the aromatic compound as measured by flash photolysis. [b] Value given here is calculated as $k_f k_d : (k_f + k_r)$ using constants from Table 5.

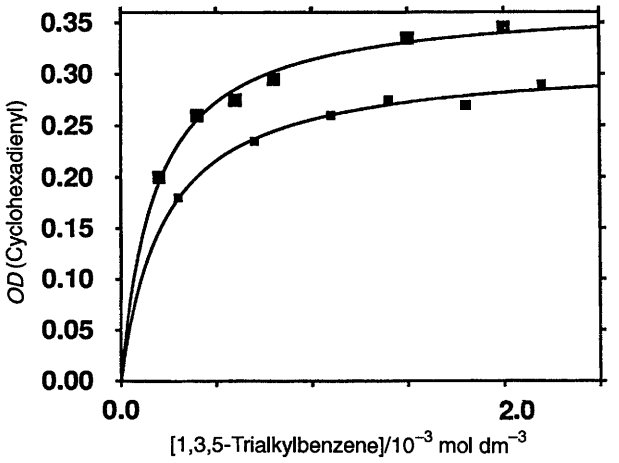

Fig. 7 Relationship between the maximum optical density at the λ_{max} of the cyclohexadienyl cation and the concentration of mesitylene (large squares) and 1,3,5-triisopropylbenzene (small squares). The points are experimental; the curve has been drawn according to eqn. (7).

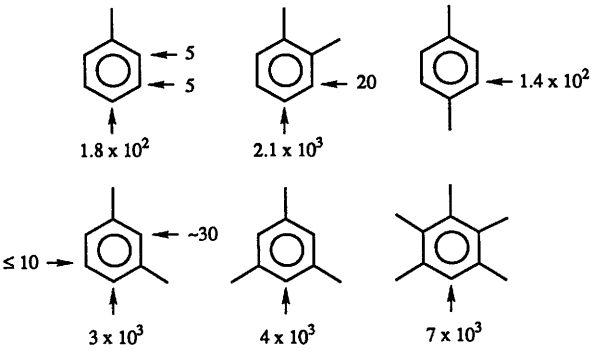

Fig. 8 Partial rate factors for substitution of Fl^+ in methylbenzenes

any further reactions occur, the differences between these pairs of rate constants should be larger. Our view is that the system can be viewed as reaching a quasi-equilibrium, at least sufficiently close to a true equilibrium that the rate and equilibrium constants that have been calculated are within 10–20% of their true values.

To verify that this is the case, an independent measurement of the equilibrium constant was obtained from the maximum absorbance of the cyclohexadienyl cation as a function of [ArH]. At the stage where equilibrium is reached, this absorbance is given by eqn. (7), where ε_{cyc} is the extinction

$$\text{Abs} = \varepsilon_{cyc} L[Fl^+]_i \left(\frac{K_{eq}[ArH]}{1 + K_{eq}[ArH]} \right) \qquad (7)$$

coefficient of the cyclohexadienyl cation, L is the path length of the cuvette, $[Fl^+]_i$ is the initial concentration of the 9-fluorenyl cation and K_{eq} is the equilibrium constant. This equation is derived making two assumptions. One is the complete equilibration of Fl^+ and the cyclohexadienyl cation before any other reaction occurs. The other is that Fl^+ makes a negligible contribution to the absorbance at the wavelength where the measurements are being made.

According to eqn. (7), measurement of the absorbance at various [ArH] can provide K_{eq} providing $[Fl^+]_i$ remains constant. In this case the experimental data can be fitted to eqn. (7) with two parameters, K_{eq} and $(\varepsilon_{cyc} L[Fl^+]_i)$. Maintaining $[Fl^+]_i$ constant was achieved by conducting flash photolysis experiments under identical conditions of laser dose and concentration of the precursor 9-fluorenol. Fig. 7 provides experimental data for two systems, with the curves drawn according to eqn. (7) and the values of the two parameters that provide the best fit. Table 5 summarizes the values of K_{eq} so obtained.

It can be seen that there is reasonable agreement between these values and the ratios $k_f : k_r$ obtained in the kinetic analyses. As we have discussed, the equilibrium between Fl^+ and the cyclohexadienyl cation is never fully attained. The consequence is that the values of K_{eq} obtained by the absorbance method are not precisely determined, since the cyclohexadienyl cations are undoubtedly undergoing some further reaction before they reach their maximum equilibrium position.

Products with benzenes bearing multiple alkyl substituents

Products were characterized with three of the alkylbenzenes of Table 4, *m*-xylene, mesitylene and pentamethylbenzene. These are summarized in Table 6, along with products from other ArH where the cyclohexadienyl cation is not observed. With *o*-xylene, the 3-position and the 4-position are almost equally activated on electronic grounds; 99% substitution, however, occurs at the 4-position. This is undoubtedly due to a steric effect, the bulky 9-flourenyl group avoiding substitution next to two adjacent methyl groups. A steric effect must also be responsible for the 99.5% yield of the 4-substituted product with *m*-xylene, where substitution between the two methyl groups is avoided. That such a substitution can occur where there is no other option is seen with mesitylene and pentamethylbenzene.

Fig. 8 shows partial rate factors for substitution of Fl^+ into methylbenzenes. These have been calculated in the standard manner on the basis of the product distributions given in Table 6 and the appropriate statistical correction factors. The ratio

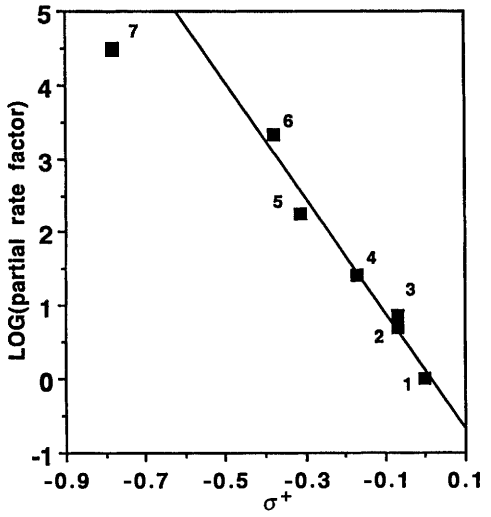

Fig. 9 Relationship between the logarithm of the partial rate factors and σ^+ for the reaction of the 9-fluorenyl cation with aromatic compounds. Points represent (**1**) parent; (**2**) *m*-methyl; (**3**) *p*-fluoro; (**4**) *p*-phenyl; (**5**) *p*-methyl; (**6**) 4-position in *o*-xylene; (**7**) *p*-methoxy. The line is based on linear regression for points (**1**)–(**6**) and has a slope of −7.8.

$k_{ArH}:k_{benzene}$ that is required in this calculation was taken as the ratio of the two values for k_{Ar}(obs), as given in the same table. There are no surprises in these numbers, except, as to be discussed later, the very high intramolecular selectivity that is observed, for example, with *m*-xylene.

Reversibility with benzene and toluene

With the alkylbenzenes in Table 5 the addition of Fl^+ to the aromatic compound is largely reversible in that the cyclohexadienyl cation reverts to Fl^+ and ArH at least twice as fast as it deprotonates. To investigate the issue of reversibility for benzene and toluene, a kinetic isotope effect has been measured. This has been done by the competition method, by photolysing 9-fluorenol (1 mmol dm^{-3}) in HFIP in the presence of an equivalent amount of benzene:[$^2H_6$]benzene (0.5 mmol dm^3 each) or toluene:[$^2H_8$]toluene (0.1 mmol dm^3 each). In the former case the peak in the GC corresponding to (9-fluorenyl)benzene was analysed by multiple measurements with GC–MS. For the latter, the peak analysed was that of *p*-(9-fluorenyl)toluene. The $k_H:k_D$ ratios were calculated directly as the ratio of molecular ions (m/z = 242:m/z = 247 for benzene, and m/z = 256:m/z = 263 for toluene).

The $k_H:k_D$ values so obtained are 1.48 ± 0.05 for benzene and 1.56 ± 0.08 for toluene. These ratios are relatively small for a primary isotope effect, but they are too large for a secondary isotope effect. They are in fact in the wrong direction for the latter. Electrophilic substitutions where formation of the cyclohexadienyl cation is fully rate limiting would be expected to show a small inverse secondary isotope effect associated with the change in hybridization from sp^2 to sp^3. The conclusion is that the deprotonation step is also rate-limiting, or at least partially so, with benzene and toluene. There is precedence for this situation in Friedel–Crafts alkylations. For example, Brown and Brady have reported $k_H:k_D$ = 1.58 for benzylation of benzene *versus* [$^2H_6$]benzene.[45]

The actual magnitudes of the observed $k_H:k_D$ values are consistent with deprotonation being entirely rate-limiting with $k_H:k_D$ for this step being considerably smaller than the maximum. The absolute rate constants obtained with the electron rich ArH suggest that this could be the case, since these show that the k_d values for the deprotonation are large, even for relatively stabilized cyclohexadienyl cations. For the less stable adducts of toluene and benzene, k_d will be even larger, probably of the order of 10^8–10^9 s^{-1}. This could mean that the transition state is very early, in which case $k_H:k_D$ would be small.

Significance of k_{Ar}(obs)

The failure to observe the cyclohexadienyl cation in the flash photolysis experiments with the less electron-rich aromatics must arise because of the very short lifetime of this intermediate. The kinetic isotope effects imply that deprotonation is at least partially rate-limiting, certainly with benzene and toluene, and likely with the others of this type. This being the case, the quantity k_{Ar}(obs) that is measured in the flash photolysis experiments with these compounds is given by eqn. (8) where the microscopic rate constants are defined in Scheme

$$k_{Ar}(\text{obs}) = k_f\left(\frac{k_d}{k_r + k_d}\right) \quad (8)$$

4. The quenching constant k_{Ar}(obs) is therefore lower than the rate constant k_f for the addition of Fl^+ to ArH. For the more electron-rich aromatics where the microscopic constants are determinable, $k_r:k_d$ is ~2, at least for most of the systems. If this same factor were to apply to those derivatives where the breakdown into the individual constants is not possible, k_f would be approximately three times the value of k_{Ar}(obs).

In terms of product ratios measured in competition experiments, the important constant is k_{Ar}(obs), not k_f. This is illustrated for the toluene:benzene competition in eqn. (9). The

$$\frac{k_{toluene}}{k_{benzene}} = \frac{[\text{(9-fluorenyl)toluenes}][\text{benzene}]}{[\text{(9-flourenyl)benzene}][\text{toluene}]} = \frac{\left(\frac{k_f k_d}{k_r + k_d}\right)_{toluene}}{\left(\frac{k_f k_d}{k_r + k_d}\right)_{benzene}} \quad (9)$$

selectivity, the term on the left, is calculated experimentally through the expression in the middle. This in turn is equivalent to the expression containing the microscopic rate constants given on the right. Thus the selectivity $k_{toluene}:k_{benzene}$ from the product analysis is equal to the ratio of quenching constants [$k_{toluene}$(obs):$k_{benzene}$(obs)] measured by flash photolysis. These ratios are indeed within experimental error of one another.

With anisole the decay of Fl^+ is strictly single exponential, but here the cyclohexadienyl cation is the product after the decay. Thus, the quantity $k_{anisole}$(obs) must in this case be equal to k_f. There is uncertainty in the fate of the cyclohexadienyl cations that are so formed, *i.e.* whether they undergo solely deprotonation or whether there is some reversibility. The lack of two-component decay argues against the latter, although a very large equilibrium constant for the Fl^+–cyclohexadienyl equilibrium would produce the experimental result of a single exponential. A competition experiment, carried out with 10^{-3} mol dm^{-3} anisole and 1.00 mol dm^{-3} benzene, provides a ratio $k_{anisole}:k_{benzene}$ = 5.8 × 10^3. The flash photolysis ratio $k_{anisole}$(obs):$k_{benzene}$(obs) is 5.2 × 10^3. The ratio calculated from the product analysis is still given by eqn. (9) (with anisole replacing toluene), while the flash photolysis ratio uses only k_f(anisole). The approximate equality of the two ratios therefore implies that the additional term in the product equation in $k_d:(k_r + k_d)$ does not make a significant contribution. Thus there is probably little reversibility of the cyclohexadienyl cations formed from anisole.

Linear free energy correlations

Fig. 9 shows the Hammett plot constructed with partial rate factors calculated from the ratio of absolute rate constants k_{Ar}(obs):$k_{benzene}$(obs) and product distributions (see Table 6 for data). The appropriate statistical corrections have been made, and the plot limited to examples where substitution has occurred in a *meta* or *para* position. The one uncertainty

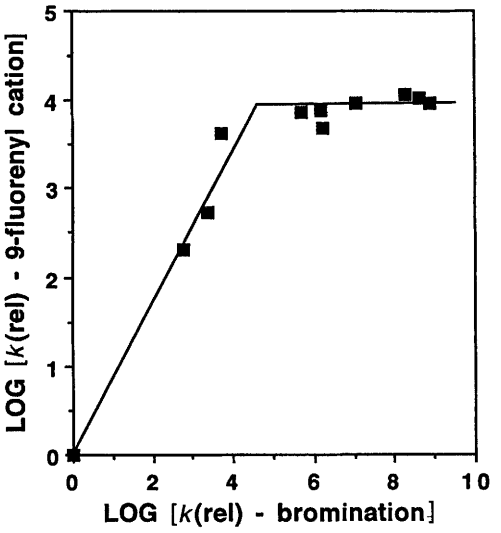

Fig. 10 Linear free energy correlation: Fl^+ + methylbenzenes in the solvent HFIP *versus* Br_2 + methylbenzenes in 85% acetic acid (ref. 47). Lines have been drawn with slopes of 0.87 and 0.

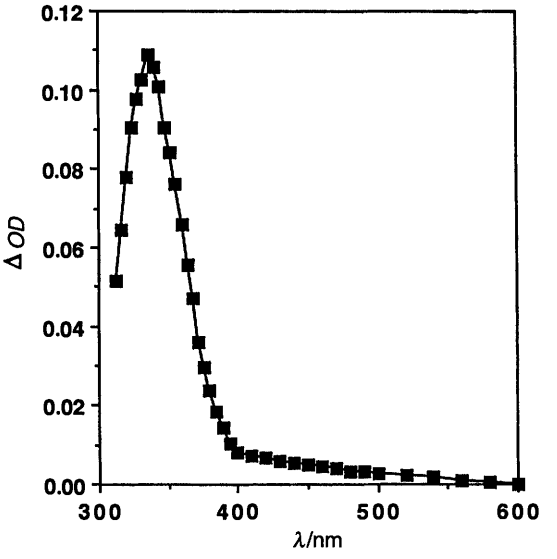

Fig. 11 Transient absorption spectrum generated upon 308 nm excitation of 9-fluorenol in HFIP in the presence of 2×10^{-3} mol dm^{-3} *p*-methoxystyrene. The spectrum shown has been obtained at a time 770 ns after irradiation, after complete decay of the 9-fluorenyl cation at 515 nm.

involves fluorobenzene where product data has not been determined; the point in Fig. 9 is based on 50% *para* substitution.

As discussed in the last section the constant k_{Ar}(obs) is a collection of microscopic rate constants [eqn. (8)]. The partitioning factor $k_d:(k_r + k_d)$ however is relatively constant for the examples where this quantity can be directly evaluated, and we assume that this is true for the systems in Fig. 9 also. Thus the variation in k_{Ar}(obs) can be attributed to changes in k_f, the rate constant for the formation of the cyclohexadienyl cation. This is obvious in the Hammett plot, which shows a reasonable linear correlation in σ^+ with a large negative ρ^+ value typical of electrophilic aromatic substitution.[46] The indication is that there is a substantial amount of positive charge in the aromatic ring in the transition state for the addition step; *i.e.* that this transition state has considerable character of the cyclohexadienyl cation.

The negative deviation observed for the anisole point in Fig. 9 can be explained through the model of reaction (10) which

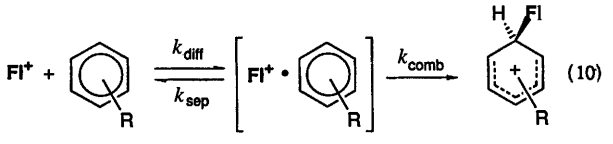

(10)

explicitly includes diffusional encounter in the addition step. For the systems that produce the linear correlation, covalent bond formation within the Fl^+–ArH complex is wholly rate limiting ($k_{sep} > k_{comb}$), and k_f reflects a large dependence on the nature of R. With the electron-rich anisole however, k_{comb} has become very fast, and diffusional encounter is partly, if not wholly, rate-limiting. In other words the deviation with anisole is caused by a change from activation-controlled formation of the cyclohexadienyl cation to diffusion-controlled formation of the encounter complex.

The dramatic nature of this change over is seen more clearly when rate constants for Fl^+ are compared with those for Br_2 (Fig. 10). The compounds here are all methylbenzenes, and for the four least reactive substrates in the set (benzene, toluene, *p*-xylene and *o*-xylene), each electrophile shows about four orders of magnitude increase in rate constant across the series. The slope of the log–log plot is 0.9, indicating that Fl^+ is slightly less selective. (Though with only four points one could argue that the selectivities are identical.) For bromination the further addition of methyl groups in positions that stabilize the cyclohexadienyl cation continues to result in rate accelerations, with a further five orders of magnitude increase from *o*-xylene to pentamethylbenzene, the most reactive compound. With Fl^+, there is little further increase. The seven most reactive compounds exhibit essentially the same reactivity, and the slope of the linear free energy correlation *versus* Br_2 is zero.

Reaction of the 9-fluorenyl cation with styrene derivatives

The conclusion that the more reactive of the aromatic compounds react with Fl^+ at (or at least very near) the diffusion limit is of course consistent with the values of k_f that have been measured for these substrates. These are all essentially the same, 1.5–2.0 $\times 10^9$ dm^3 mol^{-1} s^{-1}, and moreover are of a magnitude associated with encounter-control. Another example of a process involving Fl^+ that is clearly diffusion-controlled is its reaction with styrenes [reaction (11)]. An example of transient spectroscopy with 4-

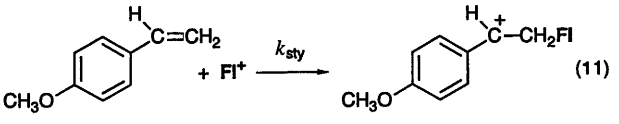

(11)

methoxystyrene is shown in Fig. 11. As with the electron-rich aromatics, decay of Fl^+ is accompanied by the growth in absorbance in the region 300–400 nm. Both the decay and the growth proceed with identical rates, an indication that the species that appears must be the product of the reaction of Fl^+. Coupling this with the λ_{max} of the new transient, 340 nm, leaves little doubt as to the assignment of this species to the β-(9-fluorenyl)-*p*-methoxyphenethyl cation, formed by addition of Fl^+ to the β-carbon of the styrene. The *p*-methoxyphenethyl cation itself is obtained by direct irradiation of *p*-methoxystyrene in both HFIP and TFE, arising *via* a photoprotonation pathway, and also has λ_{max} at 340 nm.[29,47] Further consistency in the present assignment is seen in the rate constant for the decay of the new species, $k \sim 10^2$ s^{-1}, which is slow and comparable to that of the *p*-methoxyphenethyl cation in HFIP.[29]

Similar spectral behaviour is seen when Fl^+ is generated in HFIP in the presence of *p*-methylstyrene and styrene. In each of these cases the appropriate β-(9-fluorenyl)phenethyl cation appears as Fl^+ decays. The λ_{max} and decay kinetics of this new

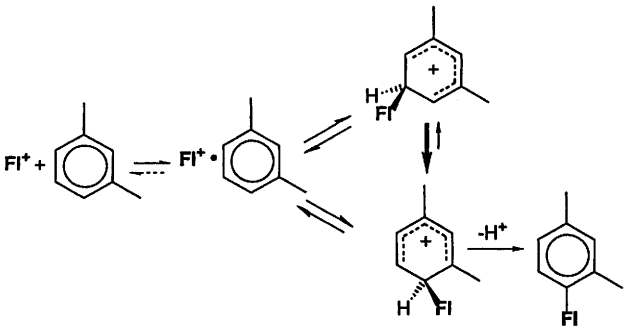

Scheme 5

cation are comparable to the protonated analogue, generated by photoprotonation in HFIP.

With all three styrenes, the decay of Fl^+ is first-order at all concentrations of the added styrene, and there is no sign of a two component decay indicative of reversibility. Plots of k_{decay} *versus* [styrene] show the expected linearity. The slopes represent k_{sty} of reaction (11), the rate constant for the addition of Fl^+ to the β-carbon. The values that are obtained are within experimental error indistinguishable, 2.6×10^9 (4-methoxy), 2.7×10^9 (4-methyl) and 3.0×10^9 dm^3 mol^{-1} s^{-1} (parent). Considering the considerable cation-stabilizing effect of the 4-methoxy substituent, the constancy must mean that these rate constants do not reflect formation of the phenethyl cation. They reflect simply the process of diffusional encounter.

Diffusion-controlled reactions with high intramolecular selectivity

There seems little doubt therefore that a rate constant of $\sim 3 \times 10^9$ dm^3 mol^{-1} s^{-1} represents diffusion-controlled combination of Fl^+ and styrenes in HFIP, while a value of ~ 2 dm^3 mol^{-1} s^{-1} applies to Fl^+ and aromatic compounds in HFIP. Such differences between rate constants for encounter-controlled cation–nucleophile combinations have been observed previously and can be explained by differences in the extent of formation of non-productive complexes.[11]

There have been suggestions that transition states in electrophilic aromatic substitutions can resemble either a σ-complex, the cyclohexadienyl cation or a π-complex.[48] The latter situation is predicted to be favoured for reactions that are very fast. The experimental characteristics are a low intermolecular selectivity, and an *ortho*:*para* ratio in toluene near 2:1. Even for the less electron-rich ArH such as benzene and toluene, the reactions with Fl^+ would have to be considered as falling into the category of being very fast. Despite this, there is still a sizable toluene:benzene selectivity and little *ortho* product with toluene. These observations therefore are inconsistent with a transition state with π-complex character and must indicate a transition state with considerable σ-complex character. We have of course previously reached this conclusion on the basis of the Hammett σ^+ correlation. The conclusion therefore is that despite the very rapid reaction, the Friedel–Crafts alkylation of benzene and toluene with Fl^+ must have significant C–C bond formation in the transition state.

What then of the reaction of Fl^+ with compounds such as pentamethylbenzene, mesitylene, *m*-xylene and anisole? Here there is little intermolecular selectivity in a comparison involving a given pair, since the rate constants k_f are all essentially the same. However there is still a large intramolecular selectivity (where this is possible), *e.g.* no *meta* product with anisole and no 5-substitution in *m*-xylene. This distinction between intermolecular selectivity and intramolecular selectivity is accounted for through the separation of the rate-determining step and the product-determining step. For the electron-rich aromatics and Fl^+, the former is diffusional encounter. Once the encounter complex has formed, the combination of Fl^+ and the aromatic compound is extremely fast, faster than diffusional separation. This combination represents the product-determining step with respect to orientation. However despite a very large rate, high intramolecular selectivity continues to be observed.

These findings are reminiscent of those for nitrations of certain alkylbenzenes which show a high intramolecular selectivity, but no intermolecular selectivity.[48–51] The commonly accepted explanation is that of Moodie and co-workers, who propose that the rate-determining step in the overall substitution is the formation of an encounter complex between NO_2^+ and the aromatic compound.[49] The product-determining step is then a fast step in which the complex converts to products by way of the cyclohexadienyl cation.

Our model for Fl^+ where diffusional encounter becomes rate-limiting is essentially the same. Flash photolysis provides direct evidence for such an interpretation, by providing the absolute rate constants for the Fl^+ addition step. These experiments also suggest a factor that may contribute to the high intramolecular selectivity once the complex is formed. Scheme 5 illustrates the features of this explanation with *m*-xylene as the substrate. Within the ion-molecule complex involving *m*-xylene, covalent bond formation can occur at three chemically distinct carbons. We argue that this combination is reversible, with the result that there is an equilibrium between the possible cyclohexadienyl cations that might form. Thus the full stability of the cyclohexadienyl cation becomes important in the determination of orientation, and large intramolecular selectivities are expected. The flash photolysis studies again provide support for this explanation, since they show with compounds like *m*-xylene that the formation of the cyclohexadienyl cation is indeed reversible.

Summary

(*a*) The 9-fluorenyl cation behaves as a normal electrophile of intermediate reactivity in terms of its intermolecular selectivity between toluene and benzene and its intramolecular selectivity within toluene.

(*b*) The photochemical route to Fl^+ permits the use of flash photolysis techniques to directly study the reaction of a benzylic-type cation with aromatic compounds. With electron-rich ArH, the cyclohexadienyl cation is observed as Fl^+ decays. Thus both cationic intermediates of a Friedel–Crafts alkylation are observed in the same experiment.

(*c*) With anisole the formation of an oxonium ion as an intermediate can be ruled out if the oxonium ion converts to the cyclohexadienyl cation by an intermolecular process. If this conversion is intramolecular, the maximum lifetime of the oxonium ion is 10 ns.

(*d*) With alkylbenzenes bearing two alkyl groups in a 1,3-relation, a two-component decay of Fl^+ demonstrates that formation of the cyclohexadienyl cation is reversible, or at least quasi-reversible. Kinetic analysis furnishes absolute rate constants for the formation of the cyclohexadienyl cation, as well as for the loss of H^+ and Fl^+ from this species. Values of $k_H:k_D$ for benzene:[$^2H_6$]benzene and toluene:[$^2H_8$]toluene are ~ 1.5 and demonstrate that Fl^+ addition is at least partly reversible with these compounds as well.

(*e*) The ρ^+ value for the 9-fluorenyl cation reacting with substituted aromatic compounds is -8, indicative of a transition state with considerable cyclohexadienyl cation character.

(*f*) The negative deviation for anisole in this plot is explained by a change to encounter control. The sharpness of this changeover is dramatically indicated in a linear free energy correlation of data for Fl^+ and Br_2. The concept of encounter control is strongly supported by the absolute rate constants for the addition step.

(*g*) Electron-rich aromatic compounds show no intermolecular selectivity, but continue to show high intramolecular selectivity. The lack of intermolecular selectivity is unambiguously demonstrated to be associated with the process being diffusion controlled. A factor in the high intramolecular selectivity is suggested to be reversibility of formation of the cyclohexadienyl cation from the encounter complex.

Experimental

9-Fluorenol was commercially available and was recrystallized before use. 1,1,1,3,3,3-Hexafluoroisopropyl alcohol was dried over 4 Å molecular sieves and distilled under nitrogen through a 40 cm Vigreux column immediately prior to use.

The authentic samples of the fluorenyl–ArH substitution products were prepared by a two-step procedure (except for pentamethylbenzene). In the first reaction 9-aryl-9-fluorenol was prepared from the reaction of fluorenone with the appropriate Grignard reagent in THF or diethyl ether. This fluorenol was then reduced to the 9-arylfluorene by reaction with solid zinc iodide and excess sodium borohydride in 1,2-dichloroethane. This procedure is exemplified by the preparation of 2-(9-fluorenyl)toluene.

9-(2-Methylphenyl)-9-fluorenol

The Grignard reagent prepared from 2.0 g of 2-bromotoluene (12 mmol) and 0.58 g of magnesium (24 mmol) in 30 cm^3 of dry diethyl ether was added to 2.0 g of fluorenone (11 mmol) in 20 cm^3 of dry benzene. After refluxing overnight, 15 cm^3 of cold 20% sulfuric acid was added. The ether–benzene layer was separated, washed with $NaHCO_3$ and dried with anhydrous $MgSO_4$. After solvent removal the material was recrystallized from ether–hexane. Mp 122–123 °C (lit.,[52] 121–123 °C).

2-(9-Fluorenyl)toluene

To a stirred solution of the above fluorenol (3.6 mmol) in 1,2-dichloroethane (50 cm^3) at room temperature were added solid zinc iodide (5.6 mmol) and sodium borohydride (52 mmol). After 24 h reflux, filtration through Celite and evaporation of the solvent, the residue was chromatographed on silica gel, eluting with 5% ethyl acetate in hexane. This gave a colourless product in 91% yield. Mp 92–93 °C (lit.,[53] 92–93.5 °C). It should be noted that the ^1H NMR spectrum of this compound is unusual, as are many of the related compounds. This has been observed previously and attributed to two different conformations that are not equilibrated on the NMR timescale.[54,55]

The following known compounds were prepared in similar reactions. 9-(3-Methylphenyl)-9-fluorenol, mp 81–83 °C (lit.,[56] 81–83.5 °C). 3-(9-Fluorenyl)toluene, mp 126–128 °C (lit.,[57] 128 °C). 9-(4-Methylphenyl)-9-fluorenol, mp 84–86 °C (lit.,[57] 85–86.5 °C). 4-(9-Fluorenyl)toluene, mp 125–127 °C (lit.,[54] 127 °C). 9-(3-Methoxyphenyl)-9-fluorenol, mp 82–83 °C (lit.,[58] 81–82 °C). 9-(4-Methoxyphenyl)-9-fluorenol, mp 97–98.5 °C (lit.,[57] 97–99 °C). 4-(9-Fluorenyl)anisole, mp 121–122 °C (lit.,[59] 121 °C). 9-(2,6-Dimethylphenyl)-9-fluorenol, mp 109–111 °C (lit.,[60] 110–112 °C). 2-(9-Fluorenyl)-1,3-dimethylbenzene, mp 86–88 °C (lit.,[61] 85–88 °C). 9-(2,5-Dimethylphenyl)-9-fluorenol, mp 98–100 °C (lit.,[55] 97–99 °C). 9-(2,4,6-Trimethylphenyl)-9-fluorenol, mp 108–110 °C (lit.,[61] 110–112 °C). 2-(9-Fluorenyl)-1,3,5-trimethylbenzene, mp 87–89 °C (lit.,[61] 85–88 °C).

The following appear to be new compounds.

9-(2-Methoxyphenyl)-9-fluorenol. Mp 106–107.5 °C. $\delta_H(CDCl_3$, 200 MHz) 2.34 (s, 1 H), 3.81 (s, 3 H), 6.81 (t, 1 H, J = 7.4 Hz), 6.92 (d, 1 H, J = 7.4 Hz), 7.09–7.39 (mult., 6 H), 7.52 (d, 2 H, J = 7.3 Hz) and 7.67 (d, 2 H, J = 7.4 Hz) (Calc. for $C_{20}H_{16}O_2$: C, 83.31; H, 5.59. Found: C, 83.29; H, 5.64%).

2-(9-Fluorenyl)anisole. Mp 81–83 °C. $\delta_H(CDCl_3$, 200 MHz) 3.84 (s, 3 H), 5.00 (s, 1 H), 6.82 (t, 1 H, J = 7.4 Hz), 6.93 (d, 2 H, J = 7.4 Hz), 7.02 (d, 1 H, J = 7.6 Hz), 7.17–7.30 (mult., 2 H), 7.37 (1 H, dt, J = 7.5 and 1.2 Hz), 7.53 (d, 2 H, J = 7.5 Hz) and 7.68 (d, 2 H, J = 7.6 Hz) (Calc. for $C_{20}H_{16}O$: C, 88.20; H, 5.92. Found: C, 88.17; H, 5.90%).

3-(9-Fluorenyl)anisole. Mp 95–96 °C. $\delta_H(CDCl_3$, 200 MHz) 3.70 (s, 3 H), 5.01 (s, 1 H), 6.62–6.72 (mult., 3 H), 7.14–7.38 (mult., 7 H) and 7.78 (d, 2 H, J = 7.4 Hz) (Calc. for $C_{20}H_{16}O$: C, 88.20; H, 5.92. Found: C, 88.02; H, 6.08%).

9-(2,4-Dimethylphenyl)-9-fluorenol. Mp 101–103 °C. $\delta_H(CDCl_3$, 200 MHz) 2.31 (s, 3 H), 2.36 (s, 1 H), 6.79 (s, 1 H), 7.15–7.26 (mult., 6 H), 7.37 (t, 2 H, J = 7.4 Hz) and 7.70 (d, 2 H, J = 7.4 Hz) (Calc. for $C_{21}H_{18}O$: C, 88.08; H, 6.34. Found: C, 87.68; H, 6.47%).

4-(9-Fluorenyl)-1,3-dimethylbenzene. Mp 79–81 °C. $\delta_H(CDCl_3$, 200 MHz) 1.01 (s, 3 H, *syn*-Me), 2.01 (s, 3 H, *anti*-Me), 2.43 (s, 3 H, *syn*-Me), 2.71 (s, 3 H, *anti*-Me), 4.96 (s, 1 H, *syn*-H), 6.17 (s, 1 H, *anti*-H), 6.85 (t, 2 H, J = 7.5 Hz), 7.17 (d, 1 H, J = 7.6 Hz), 7.20–7.30 (mult., 4 H), 7.35–7.45 (mult., 2 H) and 7.82 (d, 2 H, J = 7.5 Hz). HRMS (EI, 70 eV): m/z, 270.1411. $C_{21}H_{18}$ requires 270.1409.

9-(3,5-Dimethylphenyl)-9-fluorenol. Mp 82–83.5 °C. $\delta_H(CDCl_3$, 200 MHz) 2.26 (s, 6 H), 2.42 (s, 1 H), 6.88 (s, 1 H), 6.98 (s, 2 H), 7.19–7.40 (mult., 6 H) and 7.64 (d, 2 H, J = 2.3 Hz) (Calc. for $C_{21}H_{18}O$: C, 88.08; H, 6.34. Found: C, 88.00; H, 6.50%).

5-(9-Fluorenyl)-1,3-dimethylbenzene. Mp 144–146 °C. $\delta_H(CDCl_3$, 200 MHz) 2.24 (s, 6 H), 4.97 (s, 1 H), 6.70 (s, 1 H), 6.86 (s, 1 H), 7.27 (dt, 2 H, J = 7.4 and 1.1 Hz), 7.30–7.40 (mult., 4 H) and 7.81 (d, 2 H, J = 7.5 Hz) (Calc. for $C_{21}H_{18}$: C, 93.29; H, 6.71. Found: C, 92.96; H, 6.61%).

2-(9-Fluorenyl)-1,4-dimethylbenzene. Mp 88–90 °C. $\delta_H(CDCl_3$, 200 MHz) 1.08 (s, 3 H, *syn*-Me), 2.02 (s, 3 H, *anti*-Me), 2.44 (s, 3 H, *syn*-Me), 2.72 (s, 3 H, *anti*-Me), 4.97 (s, 1 H, *syn*-H), 5.38 (s, 1 H, *anti*-H), 6.18 (s, 1 H), 6.80–7.14 (mult., 6 H) and 7.80 (d, 2 H, J = 7.4 Hz). HRMS (EI, 70 eV): m/z, 270.1395. $C_{21}H_{18}$ requires 270.1409.

9-(2,3-Dimethylphenyl)-9-fluorenol. Mp 130–131 °C (lit.,[61] 108–111 °C). $\delta_H(CDCl_3$, 200 MHz) 1.22 (s, 3 H), 2.11 (s, 1 H), 2.97 (s, 3 H), 7.07 (t, 1 H, J = 7.5 Hz), 7.12–7.40 (mult., 8 H), 7.68 (d, 2 H, J = 7.4 Hz). HRMS (EI, 70 eV): m/z, 286.1374. $C_{21}H_{18}O$ requires 286.1358.

3-(9-Fluorenyl)-1,2-dimethylbenzene. Mp 117–119 °C. $\delta_H(CDCl_3$, 200 MHz) 1.04 (s, 3 H, *syn*-Me), 2.08 (s, 3 H, *anti*-Me), 2.40 (s, 3 H, *syn*-Me), 2.66 (s, 3 H, *anti*-Me), 4.97 (s, 1 H, *syn*-H), 5.48 (s, 1 H, *anti*-H), 6.25 (d, 1 H, J = 7.6 Hz), 6.78 (d, 1 H, J = 7.5 Hz), 7.01 (d, 1 H, J = 7.4 Hz), 7.05–7.75 (mult., 6 H) and 7.80 (d, 2 H, J = 6.5 Hz) (Calc. for $C_{21}H_{18}$: C, 93.29; H, 6.71. Found: C, 93.55; H, 6.69%).

9-(3,4-Dimethylphenyl)-9-fluorenol. Mp 112–114 °C. $\delta_H(CDCl_3$, 200 MHz) 2.24 (s, 1 H), 2.30 (s, 3 H), 2.38 (s, 3 H), 7.18 (d, 2 H, J = 7.4 Hz), 7.20–7.60 (mult., 6 H) and 7.81 (d, 2 H, J = 7.4 Hz) (Calc. for $C_{21}H_{18}O$: C, 88.08; H, 6.34. Found: C, 88.36; H, 6.12%).

4-(9-Fluorenyl)-1,2-dimethylbenzene. Mp 97–98.5 °C. $\delta_H(CDCl_3$, 200 MHz) 2.17 (s, 3 H), 2.22 (s, 3 H), 4.99 (s, 1 H), 6.85 (d, 2 H, J = 7.0 Hz), 7.02 (d, 1 H, J = 7.5 Hz), 7.20–7.40 (mult., 6 H), 7.82 (d, 2 H, J = 7.4 Hz). HRMS (EI, 70 eV): m/z, 270.1403. $C_{21}H_{18}$ requires 270.1409.

9-(4-Biphenylyl)-9-fluorenol. Mp 172–174 °C. $\delta_H(CDCl_3$, 200 MHz) 2.21 (s, 1 H), 5.96 (d, 2 H, J = 6.9 Hz), 6.58 (t, 1 H), 6.86 (d, 2 H, J = 7.4 Hz), 7.10–7.20 (mult., 6 H), 7.29–7.57 (mult., 4 H) and 8.41 (d, 2 H, J = 6.7 Hz). HRMS (EI, 70 eV): m/z, 334.1353. $C_{25}H_{18}O$ requires 334.1357.

4-(9-Fluorenyl)biphenyl. Mp 172–174 °C. $\delta_H(CDCl_3$, 200 MHz) 5.09 (s, 1 H), 5.98 (d, 2 H, J = 6.7 Hz), 6.58 (t, 2 H, J = 7.3 Hz), 6.70–6.90 (mult., 2 H), 7.10–7.62 (mult., 10 H), 8.41 (d, 2 H, J = 6.7 Hz). HRMS (EI, 70 eV): m/z, 318.1410. $C_{25}H_{18}$ requires 318.1409.

6-(9-Fluorenyl)-1,2,3,4,5-pentamethylbenzene. 9-Bromofluorene (0.5 g, 2.0 mmol) and pentamethylbenzene (0.37 g, 2.5 mmol) were added to 4 cm^3 of 1,1,1,3,3,3-hexafluoroisopropyl

alcohol at 0 °C. After 30 min standing, water (30 cm^3) was added and the mixture extracted with diethyl ether. After drying ($MgSO_4$) and removal of the ether, the residue was chromatographed on silica gel, eluting with 35% ethyl acetate in hexane, with further purification by TLC. The product was obtained as a pale yellow oil, in low yield (5%). δ_H($CDCl_3$, 200 MHz) 1.04 (s, 3 H), 2.02 (s, 3 H), 2.27 (s, 3 H), 2.38 (s, 3 H), 2.63 (s, 3 H), 5.58 (s, 1 H), 7.22 (mult., 3 H), 7.38 (mult., 3 H) and 7.88 (d, 2 H, J = 7.4 Hz). HRMS (EI, 70 eV): m/z, 312.1870. $C_{24}H_{24}$ requires 312.1878.

9-Fluorenyl 1,1,1,3,3,3-hexafluoro-2-propyl ether. 9-Bromofluorene (1 g, 4 mmol) was slowly added to 6 cm^3 1,1,1,3,3,3-hexafluoroisopropyl alcohol at 0 °C. After 60 min standing, water (30 cm^3) was added and the mixture extracted with diethyl ether. After drying ($MgSO_4$) and removal of the ether, the residue was chromatographed on silica gel, eluting with 10% dichloromethane in hexane to give a 15% yield of a white solid. Mp 107–109 °C. δ_H($CDCl_3$, 200 MHz) 4.35 (sept, 1 H), 7.35 (d, 2 H, J = 7.5 Hz), 7.44 (t, 2 H), 7.62 (d, 2 H, J = 7.4 Hz) and 7.67 (d, 2 H, J = 7.7 Hz). HRMS (EI, 70 eV): m/z, 332.0629. $C_{16}H_{10}F_6O$ requires 332.0636.

Flash photolysis experiments

9-Fluorenol (1–5 × 10^{-4} mol dm^{-3}) was dissolved in HFIP containing a known quantity of the aromatic compound and the solution irradiated at 308 nm (XeCl*) with a Lambda Physik excimer laser. Tektronix 7612 and 7912 transient recorders interfaced with a DEC LSI11/73$^+$ computer simultaneously digitized the signals. The DEC computer also controlled the operation of the apparatus, and prepared the raw experimental data for further processing. Final data analysis, such as the construction of absorption spectra and fitting of the traces was performed with a Microvax II computer. Rate constants were the average of 5–7 kinetic runs. First-order rate constants measured in freshly distilled HFIP were reproducible to ±3%. Second-order rate constants obtained as the slopes of plots of k_{obs} *versus* [ArH] had standard deviations of ±5%.

Product studies

9-Fluorenol (5–10 × 10^{-4} mol dm^{-3}) was dissolved in HFIP containing a known quantity of the aromatic compound and the solution irradiated at 300 nm in a Rayonet reactor. After various times of irradiation the solution was directly injected into a Varian 3400 gas chromatograph equipped with FID detector and DB-5 column. The qualitative characterization of the products was based upon the identity of the GC retention time with that of an authentic sample. The peak was then analysed by GC–MS to verify the assignment. For quantitative experiments, response factors were obtained by injecting known quantities of the authentic samples. Peak areas from the irradiated solutions were then converted to absolute quantities using these factors.

Acknowledgements

R. A. M. acknowledges the continued financial support of the Natural Sciences and Engineering Research Council of Canada.

References

1 D. J. Raber, J. M. Harris, R. E. Hall and P. v. R. Schleyer, *J. Am. Chem. Soc.*, 1971, **93**, 4821.
2 L. M. Stock and H. C. Brown, *Adv. Phys. Org. Chem.*, 1963, **1**, 35.
3 J. P. Richard and W. P. Jencks, *J. Am. Chem. Soc.*, 1982, **104**, 4689.
4 J. P. Richard, M. E. Rothenberg and W. P. Jencks, *J. Am. Chem. Soc.*, 1984, **106**, 1361.
5 *Carbonium Ions*, eds. G. A. Olah and P. v. R. Schleyer, New York, 1968, vol. 1; 1970, vol. 2; 1972, vol. 3; 1973, vol. 4; 1976, vol. 5.
6 P. K. Das, Chem. Rev., 1993, **93**, 119.
7 R. A. McClelland, *Tetrahedron*, 1996, **52**, 6823.
8 R. A. McClelland, V. M. Kanagasabapathy and S. Steenken, *J. Am. Chem. Soc.*, 1988, **110**, 6913.
9 R. A. McClelland, V. M. Kanagasabapathy, N. Banait and S. Steenken, *J. Am. Chem. Soc.*, 1989, **111**, 3966.
10 S. Steenken and R. A. McClelland, *J. Am. Chem. Soc.*, 1990, **112**, 9648.
11 R. A. McClelland, V. M. Kanagasabapathy, N. Banait and S. Steenken, *J. Am. Chem. Soc.*, 1991, **113**, 1009.
12 R. A. McClelland, F. L. Cozens, S. Steenken, T. L. Amyes and J. P. Richard, *J. Chem. Soc., Perkin Trans. 2*, 1993, 1717.
13 P. Wan and E. Krogh, *J. Chem. Soc., Chem. Commun.*, 1985, 1027.
14 P. Wan and E. Krogh, *J. Am. Chem. Soc.*, 1989, **111**, 4887.
15 P. Wan, E. Krogh and B. Chak, *J. Am. Chem. Soc.*, 1988, **110**, 4073.
16 R. Bolton, N. B. Chapman and J. Shorter, *J. Chem. Soc.*, 1964, 1895.
17 C. Eaborn, R. C. Golesworthy and M. N. Lilly, *J. Chem. Soc.*, 1968, 3052.
18 E. C. Friedrich and D. B. Taggart, *J. Org. Chem.*, 1978, **43**, 805.
19 T. W. Toone, E. Lee-Ruff and A. C. Hopkinson, *Can. J. Chem.*, 1975, **53**, 1635.
20 D. Bethell and V. Gold, in *Carbonium Ions. An Introduction*, Academic Press, London, 1967, pp. 76–77.
21 N. Mathivanan, R. A. McClelland and S. Steenken, *J. Am. Chem. Soc.*, 1990, **112**, 8454.
22 D. D. M. Wayner, D. J. McPhee and D. J. Griller, *J. Am. Chem. Soc.*, 1988, **110**, 132.
23 G. A. Olah, G. K. S. Prakash, G. Liang, P. W. Westerman, K. Kunde, J. Chandrasekhar and P. v. R. Schleyer, *J. Am. Chem. Soc.*, 1980, **102**, 4485.
24 S. L. Mecklenburg and E. F. Hilinski, *J. Am. Chem. Soc.*, 1989, **111**, 5471.
25 R. A. McClelland, N. Mathivanan and S. Steenken, *J. Am. Chem. Soc.*, 1990, **112**, 4857.
26 R. A. McClelland, N. Banait and S. Steenken, *J. Am. Chem. Soc.*, 1986, **108**, 7023.
27 F. L. Cozens, N. Mathivanan, R. A. McClelland and S. Steenken, *J. Chem. Soc., Perkin Trans. 2*, 1992, 2083.
28 J. E. Chateauneuf, *J. Chem. Soc., Chem. Commun.*, 1991, 1437.
29 R. A. McClelland, C. Chan, F. Cozens, A. Modro and S. Steenken, *Angew. Chem., Int. Ed. Engl.*, 1991, **30**, 1337.
30 T. L. Amyes, J. P. Richard and M. Novak, *J. Am. Chem. Soc.*, 1992, **114**, 8031.
31 F. Cozens, J. Li, R. A. McClelland and S. Steenken, *Angew. Chem., Int. Ed. Engl.*, 1992, **31**, 743.
32 F. R. Jensen and G. Goodman, in *Friedel–Crafts and Related Reactions*, ed. G. A. Olah, Wiley-Interscience, New York, 1964, vol. III, Part 2, p. 1024.
33 L. M. Stock and H. C. Brown, *Adv. Phys. Org. Chem.*, 1963, **1**, 35.
34 G. A. Olah and S. Kobayashi, *J. Am. Chem. Soc.*, 1971, **93**, 6964.
35 P. Kovacic and J. J. Hiller, *J. Org. Chem.*, 1965, **30**, 1581.
36 G. A. Olah and E. G. Melby, *J. Am. Chem. Soc.*, 1973, **95**, 4971.
37 D. A. Simpson, S. G. Smith and P. Beak, *J. Am. Chem. Soc.*, 1970, **72**, 1071.
38 N. Mathivanan, F. Cozens, R. A. McClelland and S. Steenken, *J. Am. Chem. Soc.*, 1992, **114**, 2198.
39 C. S. Q. Lew and R. A. McClelland, *J. Am. Chem. Soc.*, 1993, **115**, 11 516.
40 G. Zhang, Y. Shi, R. Mosi, T. Ho and P. Wan, *Can. J. Chem.*, 1994, **72**, 2388.
41 F. L. Cozens, R. A. McClelland and S. Steenken, *J. Am. Chem. Soc.*, 1993, **115**, 5050.
42 A. J. Kresge, Y. Chiang and L. E. Hakka, *J. Am. Chem. Soc.*, 1971, **93**, 6167.
43 G. Dalinga, E. L. Mackor and A. A. Verrijn Stuart, *Mol. Phys.*, 1958, **1**, 123.
44 V. A. Koptyug, *Top. Curr. Chem.*, 1984, **122**, 96.
45 H. C. Brown and J. D. Brady, *J. Am. Chem. Soc.*, 1952, **74**, 3570; 1959, **81**, 5611.
46 H. C. Brown and Y. Okamoto, *J. Am. Chem. Soc.*, 1958, **80**, 4979.
47 R. A. McClelland, F. Cozens and S. Steenken, *Tetrahedron Lett.*, 1990, **31**, 2821.
48 G. A. Olah, *Acc. Chem. Res.*, 1971, **4**, 240.
49 J. W. Barnett, R. B. Moodie, K. Schofield and J. B. Weston, *J. Chem. Soc., Perkin Trans. 2*, 1975, **2**, 648.
50 G. A. Olah and S. Kobayashi, *J. Am. Chem. Soc.*, 1971, **93**, 6964.
51 G. A. Olah, S. C. Narang, J. A. Olah, R. L. Pearson and C. A. Cupas, *J. Am. Chem. Soc.*, 1980, **102**, 3507.
52 L. Weiss and P. A. Knapp, *Monatsh.*, 1932, **61**, 61.
53 A. L. Wilds, R. L. Trebra and N. F. Woolse, *J. Am. Chem. Soc.*, 1969, **34**, 2401.

54 S. Tukada and T. Iwamura, *J. Chem. Soc.*, 1961, 3052.
55 T. H. Siddall and W. E. Stewart, *J. Org. Chem.*, 1969, **34**, 233.
56 A. Mathieu, *Bull. Soc. Chim. Fr.*, 1971, 1526.
57 C. Eaborn, R. C. Golesworthy and M. N. Lilly, *J. Chem. Soc.*, 1961, 3052.
58 A. F. Cockerill and J. E. Lamper, *J. Chem. Soc.* (*B*), 1971, 503.
59 R. Bolton, N. B. Chapman and J. Shorter, *J. Chem. Soc.*, 1964, 1896.
60 E. A. Chandross and C. F. Shelley, *J. Am. Chem. Soc.*, 1968, **90**, 4345.
61 K. Albert and A. Ricker, *Chem. Ber.*, 1977, **110**, 1804.

Paper 6/02508K
Received 10*th April* 1996
Accepted 26*th April* 1996